HHS Public Access

Author manuscript

Circ Cardiovasc Imaging. Author manuscript; available in PMC 2024 October 05.

Published in final edited form as:

Circ Cardiovasc Imaging. 2023 October ; 16(10): e015735. doi:10.1161/CIRCIMAGING.123.015735.

Atrial myopathy quantified by speckle-tracking echocardiography in mice

Michael J. Zhang, MD, PhD[a,b,c,*,†], **Dylan J. Gyberg, BA**[a,*], **Chastity L. Healy, BS**[a], **Naixin Zhang, MS**[a], **Hong Liu, MD, PhD**[b,c], **Samuel C. Dudley Jr., MD, PhD**[b,c], **Timothy D. O'Connell, PhD**[a,†]

[a]Department of Integrative Biology and Physiology, University of Minnesota, Minneapolis, MN

[b]Department of Medicine, Cardiovascular Division, University of Minnesota, Minneapolis, MN

[c]Lillehei Heart Institute, University of Minnesota, Minneapolis, MN

Abstract

Background: Emerging evidence suggests that atrial myopathy may be the underlying pathophysiology that explains adverse cardiovascular outcomes in heart failure and atrial fibrillation (AF). Lower left atrial (LA) function (strain) is a key biomarker of atrial myopathy, but murine LA strain has not been described, thus limiting translational investigation. Therefore, the objective of this study was to characterize LA function by speckle-tracking echocardiography in mouse models of atrial myopathy.

Methods: We used three models of atrial myopathy in wildtype male and female C57Bl6/J mice: 1) aged to 16 months; 2) angiotensin II infusion (AngII); and 3) high-fat diet + L-NAME (HFpEF). LA reservoir, conduit, and contractile strain were measured using speckle-tracking echocardiography from a modified parasternal long-axis window. Left ventricular (LV) systolic and diastolic function and global longitudinal strain were also measured. Transesophageal rapid atrial pacing was used to induce AF.

Results: LA reservoir, conduit, and contractile strain were significantly reduced in aged, AngII and HFpEF mice compared to young controls. There were no sex-based interactions. LV diastolic function and global longitudinal strain were lower in aged, AngII and HFpEF mice, but LV ejection fraction was unchanged. AF inducibility was low in young mice (5%), moderately higher in aged mice (20%), and high in AngII (75%) and HFpEF (83%) mice.

Conclusion: Using speckle-tracking echocardiography, we observed reduced LA function in established mouse models of atrial myopathy with concurrent AF inducibility, thus providing the field with a timely and clinically relevant platform for understanding the pathophysiology and discovery of novel treatment targets for atrial myopathy.

Graphical Abstract

[†]co-corresponding authors Address for correspondence: Timothy D. O'Connell, PhD, Department of Integrative Biology and Physiology, University of Minnesota Medical School, 3-141 CCRB, 2231 6th Street SE, Minneapolis, MN 55414, tdoconne@umn.edu; -and-, Michael J. Zhang, MD, PhD, Lillehei Heart Institute, Department of Medicine – Cardiovascular Division, University of Minnesota Medical School, Mayo Mail Code 508, 420 Delaware St SE, Minneapolis, MN 55455, mjzhang@umn.edu.

[*]co-first authors

Disclosures: The authors have nothing to disclose.

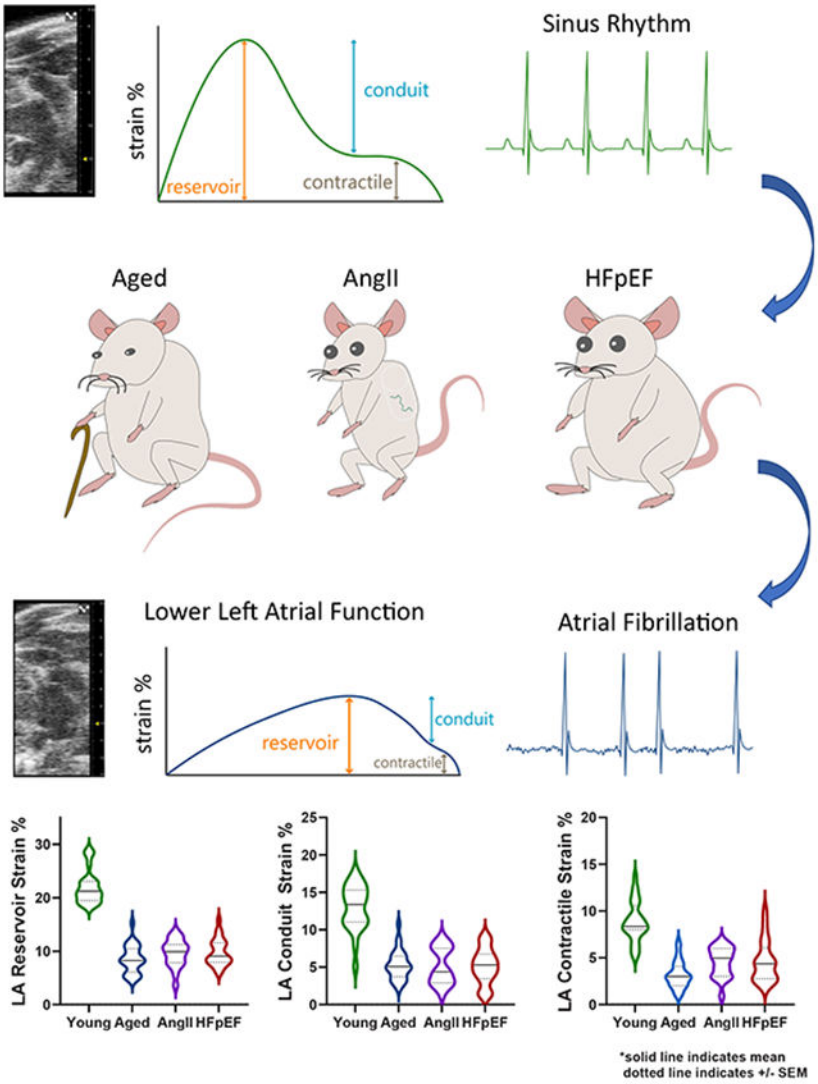

Keywords

atrial myopathy; atrial fibrillation; HFpEF; mouse models; speckle-tracking echocardiography

Journal Subject Terms

Animal Models of Human Disease; Translational Studies

Introduction

The left atrium (LA) is a significant contributor to mechanical and electrical cardiac function: 1) it serves as a reservoir for pulmonary venous return during ventricular systole; 2) it is a conduit for arterial blood during early ventricular diastolic filling; 3) it is a contractile pump to augment late diastolic filling of the ventricle; and 4) it transmits sinoatrial impulses for atrial systole.[1,2] Hence, the emerging clinical entity of atrial

myopathy, defined as “structural, architectural, contractile, or electrophysiological changes affecting the atria with the potential to produce clinically relevant manifestations”, may be a significant contributor to the heart failure (HF) exacerbations, ischemic stroke, and all-cause mortality associated with HF and atrial fibrillation (AF).[3-5] Increasing recognition of its clinical significance has thus prompted further investigation into pathophysiology of atrial myopathy.[6,7]

Murine models are essential preclinical platforms for the investigation of cardiovascular pathophysiology and multiple models of atrial myopathy have been developed in mice including: 1) aging mice to two years;[8,9] 2) infusion of high dose angiotensin II (AngII) via osmotic minipumps for three weeks;[10,11] 3) ten weeks of 60% kcal high-fat diet feeding and *N*ω-nitro-$_L$-arginine methyl ester (L-NAME) supplied in the drinking water to induce heart failure with preserved ejection fraction (HFpEF).[12] Manifestations of atrial myopathy in these models include increased atrial size, atrial fibrosis, and AF inducibility with rapid atrial pacing. However, studies characterizing or utilizing these murine models of atrial myopathy have not examined atrial function, a critical knowledge gap. Therefore, the aim of this study was to measure LA function in mice by developing a novel application of speckle-tracking echocardiography.

Methods

The data that support the findings of this study are available from the corresponding author upon reasonable request.

Animal Models

This study was carried out with adherence to the NIH Guidelines on the Use of Laboratory Animals, Animals in Research: Reporting In Vivo Experiments guidelines,[13] and all procedures were reviewed and approved by the Institutional Animal Care and Use Committee at the University of Minnesota. Four groups of wildtype, male and female C57BL/6J mice were randomly assigned and included in this study: 1) young mice (2-4 months old); 2) aged mice (16-17 months-old); 3) AngII mice (3 months old); 4) HFpEF mice (4-5 months old). Aged mice were fed normal rodent chow *ad libitum*. AngII mice underwent subcutaneous implantation of osmotic minipumps (Alzet model 1004), in the upper back between the scapulae, under isoflurane anesthesia, at 8-10 weeks of age. AngII was infused at a rate of 2 μg/kg/min.[10] HFpEF mice were maintained on a 60% kcal high fat diet (Research Diets D12492) and 0.5g/L L-NAME in the drinking water (pH increased to 7.4 with sodium hydroxide) for 10 weeks, starting at 8-10 weeks of age.[12] Systolic blood pressure was measured by tail cuff (CODA, Kent Scientific). No enrolled mice were excluded from this study.

Echocardiography

All echocardiograms were captured using an Vevo 2100 imaging system (Fujifilm, Toronto, CA) equipped with an 18-38 mHz linear array transducer. Mice were sedated with a nose cone delivering 0.5-2% inhaled isoflurane that was adjusted to maintain a heart rate between 375-450 bpm. Time-gated 2D cine loops were acquired from parasternal long

axis, parasternal short axis and apical four chamber views. The standard murine parasternal long axis window demonstrating the left ventricular outflow tract was shifted slightly to the left (i.e. modified parasternal long axis view) to reveal the LA. The sector width was narrowed when capturing cine loops of the LA to optimize frame rates. Left ventricular (LV) diastolic function was measured by obtaining E/A and E/e' ratios using pulsed wave Doppler and tissue Doppler, respectively, from the apical four chamber view. LV systolic function was quantified by measuring LV ejection fraction by averaging ejection fraction obtained from 2D edge-tracking (LV Trace) and Simpson's method of disks.[14] LV global longitudinal strain was obtained using the VevoStrain speckle-tracking software package from the parasternal long axis view.[15] Right ventricular systolic pressure (RVSP) was calculated based on the formula RVSP = −83.7 x (pulmonary artery acceleration time/ejection time) + 64.5.[16] Pulmonary artery acceleration time and ejection time were measured from the parasternal short axis window using pulsed wave Doppler of the pulmonary trunk. All echocardiographic measurements were performed by the same two operators; blinding was not possible due to the differences in animal body mass.

Left Atrial Strain Measurement

LA strain was measured using vendor-dependent speckle-tracking software (Vevo Strain within Vevo Lab version 5.7). The default period selection of R-R intervals was preserved to calculate LA strain with an end-diastolic zero reference. A minimum of three periods were selected. At the next screen, the Long Axis tool was selected (unchecking the Endo+Epi box) and a continuous line was manually defined along the endocardial LA border between the anterior and posterior mitral annulus while traversing the pulmonary veins. Based on the manually defined line, the speckle-tracking algorithm then placed 49 total points along this line, spread across six segments, and calculated global longitudinal strain. The Time-to-Peak analysis tool was then used to display the average strain curve of all six segments. LA reservoir strain was defined as the peak longitudinal strain of the averaged curve. LA contractile strain was defined as the onset of atrial contraction until end diastole and identified by the second smaller peak of the LA longitudinal strain curve. LA conduit strain is then calculated as the difference between LA reservoir strain and LA contractile strain. LA conduit and contractile strain have negative values but the absolute value is reported in this study per American Society of Echocardiography recommendations. All strain measurements were performed by a single operator blinded to the mouse group. Intra-observer variability was assessed randomly in ten measurements and variability was calculated using the individual standard deviation method.[17] Relative intraobserver and interobserver variability of LA reservoir strain was 6.54% and 8.78%, respectively.

Transesophageal Rapid Atrial Pacing

Mice were anesthetized with 2% inhaled isoflurane in O_2 flowing at 2 L/min. Two sets of surface electrocardiographic leads were inserted subcutaneously (forelimbs and lower abdomen). An 18-gauge angiocatheter was inserted into the esophagus to guide and protect the pacing catheter. Then the pacing catheter (Millar EPR-800) was advanced into the esophagus. LA capture was first confirmed by eight cycles of atrial burst pacing. After confirmation of atrial capture, decremental pacing (starting at 40 millisecond cycle length and decreasing 2 milliseconds after 50+3 cycles per decrement, initial pulse width of 5ms

and decreasing by 1ms every 3 cycles) was performed to induce AF.[10] AF inducibility was defined as the presence of irregular R-R intervals without discernable P waves for a period longer than 2 seconds. All pacing studies were conducted between 9:00 and 13:00 local time.

Statistical Analysis

Statistical analysis was performed using Prism v9 (GraphPad). Data were presented as mean ± standard error of the mean (mean±SEM). We used a two-way ANOVA with Tukey's multiple comparisons post-test to test for an interaction between sex and each outcome variable, however, we found no primary interaction between sex and any of the outcome variables. Therefore, data for each outcome was tested separately for both sexes using a one-way ANOVA with Tukey's multiple comparisons test. We used Fisher's exact test to calculate *P* values for AF inducibility. A *P* value < 0.05 was considered significant.

Results

Current methods of examining the LA are inadequate

The most widely adopted method for measuring the LA in mice using echocardiography is adapted from the clinical method of measuring a linear anteroposterior LA dimension in the parasternal long axis view (Figure 1A). However, the mouse heart has a more counterclockwise rotation (in the short axis) compared to humans, and therefore the cardiac structures imaged deep to the LV in the parasternal long axis view are not the LA but actually the basal inferior RV and RA. Instead, by shifting the ultrasound probe laterally 2-3 mm, the overlaying LV outflow tract is bypassed and a more comprehensive view of the LA can be visualized (Figure 1B, C). Although the current clinical convention of measuring LA volume and LA strain is performed in the apical four chamber and two chamber windows, this is not currently feasible in mice. This is because of the large size of the ultrasound probe relative to the size of the mouse thorax, which limits the degree by which the ultrasound probe can be rotated. This limits the ability to continuously capture the LA during both atrial systole and atrial diastole for speckle-tracking (Figure 1D, E).

Measurement of LA function in mice by speckle-tracking echocardiography

To overcome these limitations, we devised a novel approach using the modified parasternal long axis view (Figure 1C) to capture the LA clearly and continuously throughout the cardiac cycle. Representative images and videos of the focused, modified parasternal long axis view of a normal LA and dysfunctional LA are presented in Figure 2A, 2B, Video 1, and Video 2. Representative images of the R-R strain measurement gating, and speckle-tracking analysis windows are presented in Figure 2C, 2D, and 2E. Representative strain curves of a normal LA and dysfunctional LA are presented in Figure 2F and 2G.

LA function

LA reservoir strain (Figure 3A), LA conduit strain (Figure 3B), and LA contractile strain (Figure 3C) were significantly reduced in aged, AngII and HFpEF mice compared to young mice. LA stiffness index (Figure 3D), which integrates LA function with LV diastolic

function ([E/e']/[LA reservoir strain]),[18] was significantly increased in aged, AngII and HFpEF mice compared to young mice.

LV function

LV diastolic dysfunction, assessed by E/'e and E/A ratios, was evident in aged, AngII and HFpEF mice compared to young control mice. E/e' was significantly increased and e' was significantly decreased in all three groups compared to young mice (Figure 4A, 4B), whereas E/A was increased only in HFpEF mice (Figure 4C). LV global longitudinal strain was significantly reduced in aged, AngII and HFpEF mice compared to young mice (Figure 4D), although LV ejection fraction was similar in all groups (Figure 4E). Systolic blood pressure was significantly increased in AngII (males only) and HFpEF mice (males and females) but not aged mice, compared to young mice (Figure 4F). Right ventricular systolic pressure was mildly, but significantly, increased in AngII and HFpEF mice (Figure 4G). Finally, heart rates at the time of echocardiography (LV and LA parasternal long axis view) were similar in all groups (Figure 4H).

AF inducibility

AF inducibility was assessed in all mice by transesophageal rapid atrial pacing. Figure 5A displays a sample tracing that demonstrates the end of rapid atrial pacing, development of AF (lack of discernable P waves and irregular R-R intervals) and the subsequent reversion to sinus rhythm. After rapid atrial pacing, 20% of the aged males, 70% of AngII males, and 75% of HFpEF males developed AF, but none of the young males developed AF (Figure 5B). In females, 13% of the aged, 80% of AngII and 92% of HFpEF animals developed AF after rapid atrial pacing and only 9% of the young females developed AF (Figure 5B).

Discussion

In summary, we have developed a novel application of speckle-tracking echocardiography to measure LA function in mice. We demonstrated that compared to young mice, LA reservoir, conduit, and contractile function were reduced in aged, AngII, and HFpEF mice. LV diastolic and systolic dysfunction were also evident in aged, AngII, and HFpEF mice, despite having a preserved LV ejection fraction. Interestingly, AF inducibility was higher in AngII and HFpEF mice but not aged mice. This underscores the need to define LA function in preclinical models as another measure of atrial myopathy in addition to AF inducibility and atrial fibrosis.

Many previous studies have characterized the murine left atrium. Colazzo *et al.* described quantification of two-dimensional LA volume from the apical four chamber view using Simpson's rule and calculated phasic volumetric LA function.[19] However, the echocardiographic view of the orthogonal LA plane used to derive the second dimension required for Simpson's rule was undefined. Furthermore, the only cardiovascular pathology examined was in mice subject to coronary artery ligation. Medrano and Granillo *et al.* later examined LA volume in aged mice, by measuring LA size in the standard parasternal long axis view in one plane and in the parasternal short axis view for the second plane.[20,21] However, the investigators did not examine LA function nor other mouse models with

LA pathology. Hence, our study advances the field by demonstrating the feasibility of measuring murine LA function using speckle-tracking echocardiography and characterizing LA dysfunction in multiple models of atrial myopathy.

A large body of clinical data supports the importance of lower LA strain as a biomarker for atrial myopathy.[22,23] The feasibility of using echocardiographic LA strain to evaluate LA mechanical function was first demonstrated by Sirbu *et al.* in healthy humans in 2006,[24] and corroborated by Cameli and Wianna-Pinton *et al.* in 2009.[25,26] Subsequent studies demonstrated lower LA strain in patients with HF and AF.[27-29] Because invasive pressure-catheter characterization in HF and AF patients identified impaired LA mechanical function,[30,31] and histologic studies in HF and AF patients revealed significant atrial fibrosis,[32,33] LA strain has emerged as a key surrogate biomarker for the mechanical and electrophysiological abnormalities of the LA in HF and AF patients that is now collectively known as atrial myopathy.[34] Despite this emerging recognition of the importance of LA reservoir strain, the feasibility of obtaining this echocardiographic measure in mice has not been established until now.

Clinical guidelines have yet to define a consensus normal range for LA strain in humans, but the murine LA strain values in this study were comparably lower than studies in humans. A meta-analysis by Pathan *et al* in 2017 found that mean human LA reservoir strain across 40 studies was 39.4% (95% CI, 38.0%-40.8%),[35] and a recent international, multicenter, observational, World Alliance of Societies of Echocardiography study of participants without previous cardiac disease found the mean human LA reservoir strain was 42.1 ± 10%.[36] Whereas in this study, the mean murine LA reservoir strain was 22 ± 1%. Furthermore, in a cohort of TOPCAT trial participants with HFpEF, mean LA reservoir strain was 25.9 ± 7.7%,[37] whereas in this study, the mean murine LA reservoir strain in the HFpEF group was 10 ± 1%. The mean LV global longitudinal strain in the young mice of this study was also lower than normal LV global longitudinal strain values in humans, but our mean values are comparable to other murine studies.[15,38] Nevertheless, because the mean LA reservoir strain values in the mouse groups with atrial myopathy were approximately half of the value of young (normal) mice, the decrease in strain was proportional to decreases seen in humans studies. Furthermore, Matsiukevich et al recently characterized a murine model of HFpEF using combined angiotensin II and phenylephrine infusion and found a LV global longitudinal strain to LA reservoir strain ratio of 25%/40% = 0.63 in the untreated mice.[39] The LV/LA ratio in our study was similar at 15%/22% = 0.68. This concordance underscores the robustness of LA strain measurement in mice.

In addition to LA function, we also examined LV function to contextualize the interrelation of the two chambers. The AngII and HFpEF mouse models have well-characterized evidence of elevated LV filling pressures and confirmed by elevated mitral valve Doppler measurements (E/e', E/A) in our study. When the LA is exposed to elevated LV filling pressure, LA filling pressure and wall tension also increase, leading to increased LA stiffness and decreased LA compliance.[40] Because the LA is a thinner wall structure than the LV, it is more susceptible to pressure overload and remodeling occurs earlier in the LA than the LV.[23] The LA stiffness index ([E/e']/[LA reservoir strain]) was developed as a measure to directly compare LA function with LV diastolic function.[41] In our study, all three animal

models demonstrated increased LA stiffness index compared to young controls, indicating the presence of LA dysfunction in addition to LV diastolic dysfunction. Notably, recent clinical evidence has suggested that LA stiffness index is associated with adverse outcomes in HFpEF patients and has better prognostic performance compared to LV filling pressure measures.[18]

Although this study was not designed to investigate the pathophysiology of atrial myopathy in the three presented models, mechanistic insights have been suggested in prior studies. In AngII mice, the primary mechanism leading to atrial myopathy is most likely hypertension; systolic blood pressures in AngII mice were approximately 30 mmHg higher than untreated mice. In humans, increased arterial stiffness (a direct measure of hypertension) was associated with decreased LA reservoir and conduit strain.[40] Other mechanisms include oxidation and pathological activation of Ca^{2+}/calmodulin-dependent protein kinase II,[10] and direct activation of collagen deposition by cardiac fibroblasts.[42] In HFpEF mice, hypertension from L-NAME treatment is likely to be a primary mechanism for atrial myopathy, although the increase of systolic blood pressures is less than in AngII mice. Therefore, other mechanisms such as decreased AMP kinase activity and increased inflammation from the high fat diet may be important secondary contributors to atrial myopathy.[12,43,44] Consistent with other studies,[45,46] the aged mice in our study did not have hypertension, but aged mice have also been shown to have endothelial dysfunction and increased atrial fibrosis.[8,9,47] These are likely mechanisms that contribute to atrial myopathy in aged mice.

AF inducibility was high in AngII and HFpEF mice, but lower in aged mice. Nevertheless, the observed rate of AF inducibility in aged mice was consistent with other studies.[9,48] Potentially, the degree of atrial fibrosis in aged mice was insufficient to promote the substrate to induce AF.[33,49] The total collagen content measured by hydroxyproline assay in aged mice is approximately twice the content of young mice.[9] Fu *et al* compared multiple mouse models with atrial fibrosis, including transverse aortic constriction, angiotensin II infusion, and liver kinase B knockout, and found AF inducibility only with extensive atrial fibrosis (quadruple that of control).[50] Thus, our rapid atrial pacing results further underscore the need to characterize LA mechanical dysfunction (using LA reservoir strain) in mouse models, because in the clinical spectrum of atrial myopathy and AF, atrial fibrosis, and LA mechanical dysfunction usually precede the development of clinical AF.[6] Focusing preclinical investigation on mouse models with inducible AF may thus bias towards targeting a phenotype that corresponds with permanent AF in humans, a late stage that is less amenable to reverse (salutary) remodeling. Instead, using LA reservoir strain as an experimental endpoint can inform conclusions of preclinical therapeutic studies, with clinical relevance to atrial myopathy or subclinical AF, that ameliorate the development of the abnormal atrial substrate that precipitates clinical AF.

Limitations

First, we did not measure LA volume because physical limitations of currently available ultrasound probes preclude acquisition of biplane two-dimensional LA sizes in the apical views. Therefore, any estimation of LA volume based on single plane two-dimensional LA

size relies on geometric assumptions that remain unvalidated. Instead, we have focused on LA strain, because it is a better predictor of adverse cardiac events than LA volume.[51] Second, the current speckle-tracking algorithm is vendor-dependent and originally designed for the LV. Broad adoption of LA strain measurement will likely require dedicated LA-focused software. Third, there is more heterogeneity in LA strain curves than LV strain curves. This is primarily due to using the modified long axis view which sometimes reveals the left pulmonary vein, and speckle-tracking across this junction sometimes results in strain curve heterogeneity. However, this remains the best echocardiographic view because there are technical challenges to continuously visualizing the LA in apical views for speckle-tracking. Fourth, we did not examine the LA histologically for fibrosis, a substrate for AF inducibility, because this data has been demonstrated by other studies and the aim of this study was to characterize the LA noninvasively. Fifth, isoflurane anesthesia was required to sedate mice sufficiently to perform echocardiography measurements, and heart rates below 400 may not be reflective of the normal physiologic state and therefore bias LA and LV function measurements. However, both HFpEF and aged mice were obese, and obesity increases the volume of distribution of lipophilic isoflurane and complicates the rapid titration of isoflurane concentration.[52] The allowance of heart rates below 400 (down to 375) was necessary for the feasibility of echocardiography in obese mice, although our mean heart rate during echocardiography was approximately 425 (Figure 4H).

Overall, our study described a novel application of speckle-tracking echocardiography to measure LA function in mouse models and demonstrated lower LA function in established mouse models of atrial myopathy with concurrent AF inducibility. Establishment of this method provides the field with a timely and clinically relevant model for understanding the pathophysiology and discovery of novel treatment targets for atrial myopathy. Future studies should examine longitudinal changes in LA function and AF inducibility to determine if LA dysfunction is a precursor to AF to reveal mechanistic insights into the pathophysiology of atrial myopathy.

Supplementary Material

Refer to Web version on PubMed Central for supplementary material.

Acknowledgements:

This study was carried out in adherence to the NIH Guidelines on the Use of Laboratory Animals, and all procedures were approved by the University of Minnesota Committee on Animal Care.

Sources of Funding:

This work was supported by the National Institutes of Health (R01-HL152215 to T.D. O'Connell; F32-HL152523 to M.J. Zhang) and the American Heart Association (899027 to M.J. Zhang).

Nonstandard abbreviations:

AngII	angiotensin I
AF	atrial fibrillation

HFpEF	heart failure with preserved ejection fraction
L-NAME	*N*ω-nitro-$_L$-arginine methyl ester
LA	left atrial
LV	left ventricular
RVSP	right ventricular systolic pressure

References:

1. Hoit BD. Left atrial size and function: role in prognosis. J Am Coll Cardiol. 2014;63:493–505. doi: 10.1016/j.jacc.2013.10.055 [PubMed: 24291276]
2. Hoit BD, Shao Y, Gabel M, Walsh RA. In vivo assessment of left atrial contractile performance in normal and pathological conditions using a time-varying elastance model. Circulation. 1994;89:1829–1838. doi: 10.1161/01.cir.89.4.1829 [PubMed: 8149549]
3. Goette A, Kalman JM, Aguinaga L, Akar J, Cabrera JA, Chen SA, Chugh SS, Corradi D, D'Avila A, Dobrev D, et al. EHRA/HRS/APHRS/SOLAECE expert consensus on atrial cardiomyopathies: Definition, characterization, and clinical implication. Heart Rhythm. 2017;14:e3–e40. doi: 10.1016/j.hrthm.2016.05.028 [PubMed: 27320515]
4. Kamel H, Bartz TM, Elkind MSV, Okin PM, Thacker EL, Patton KK, Stein PK, deFilippi CR, Gottesman RF, Heckbert SR, et al. Atrial Cardiopathy and the Risk of Ischemic Stroke in the CHS (Cardiovascular Health Study). Stroke. 2018;49:980–986. doi: 10.1161/STROKEAHA.117.020059 [PubMed: 29535268]
5. Carlisle MA, Fudim M, DeVore AD, Piccini JP. Heart Failure and Atrial Fibrillation, Like Fire and Fury. JACC Heart Fail. 2019;7:447–456. doi: 10.1016/j.jchf.2019.03.005 [PubMed: 31146871]
6. Goldberger JJ, Arora R, Green D, Greenland P, Lee DC, Lloyd-Jones DM, Markl M, Ng J, Shah SJ. Evaluating the Atrial Myopathy Underlying Atrial Fibrillation: Identifying the Arrhythmogenic and Thrombogenic Substrate. Circulation. 2015;132:278–291. doi: 10.1161/CIRCULATIONAHA.115.016795 [PubMed: 26216085]
7. Shen MJ, Arora R, Jalife J. Atrial Myopathy. JACC Basic Transl Sci. 2019;4:640–654. doi: 10.1016/j.jacbts.2019.05.005 [PubMed: 31768479]
8. Luo T, Chang CX, Zhou X, Gu SK, Jiang TM, Li YM. Characterization of atrial histopathological and electrophysiological changes in a mouse model of aging. Int J Mol Med. 2013;31:138–146. doi: 10.3892/ijmm.2012.1174 [PubMed: 23135407]
9. Jansen HJ, Moghtadaei M, Mackasey M, Rafferty SA, Bogachev O, Sapp JL, Howlett SE, Rose RA. Atrial structure, function and arrhythmogenesis in aged and frail mice. Sci Rep. 2017;7:44336. doi: 10.1038/srep44336 [PubMed: 28290548]
10. Purohit A, Rokita AG, Guan X, Chen B, Koval OM, Voigt N, Neef S, Sowa T, Gao Z, Luczak ED, et al. Oxidized Ca(2+)/calmodulin-dependent protein kinase II triggers atrial fibrillation. Circulation. 2013;128:1748–1757. doi: 10.1161/CIRCULATIONAHA.113.003313 [PubMed: 24030498]
11. Jansen HJ, Mackasey M, Moghtadaei M, Belke DD, Egom EE, Tuomi JM, Rafferty SA, Kirkby AW, Rose RA. Distinct patterns of atrial electrical and structural remodeling in angiotensin II mediated atrial fibrillation. J Mol Cell Cardiol. 2018;124:12–25. doi: 10.1016/j.yjmcc.2018.09.011 [PubMed: 30273558]
12. Tong D, Schiattarella GG, Jiang N, Daou D, Luo Y, Link MS, Lavandero S, Gillette TG, Hill JA. Impaired AMP-Activated Protein Kinase Signaling in Heart Failure With Preserved Ejection Fraction-Associated Atrial Fibrillation. Circulation. 2022;146:73–76. doi: 10.1161/CIRCULATIONAHA.121.058301 [PubMed: 35858165]
13. Kilkenny C, Browne WJ, Cuthill IC, Emerson M, Altman DG. Improving bioscience research reporting: the ARRIVE guidelines for reporting animal research. PLoS Biol. 2010;8:e1000412. doi: 10.1371/journal.pbio.1000412 [PubMed: 20613859]

14. Zacchigna S, Paldino A, Falcao-Pires I, Daskalopoulos EP, Dal Ferro M, Vodret S, Lesizza P, Cannata A, Miranda-Silva D, Lourenco AP, et al. Towards standardization of echocardiography for the evaluation of left ventricular function in adult rodents: a position paper of the ESC Working Group on Myocardial Function. Cardiovasc Res. 2021;117:43–59. doi: 10.1093/cvr/cvaa110 [PubMed: 32365197]
15. Bauer M, Cheng S, Jain M, Ngoy S, Theodoropoulos C, Trujillo A, Lin FC, Liao R. Echocardiographic speckle-tracking based strain imaging for rapid cardiovascular phenotyping in mice. Circ Res. 2011;108:908–916. doi: 10.1161/CIRCRESAHA.110.239574 [PubMed: 21372284]
16. Thibault HB, Kurtz B, Raher MJ, Shaik RS, Waxman A, Derumeaux G, Halpern EF, Bloch KD, Scherrer-Crosbie M. Noninvasive assessment of murine pulmonary arterial pressure: validation and application to models of pulmonary hypertension. Circ Cardiovasc Imaging. 2010;3:157–163. doi: 10.1161/CIRCIMAGING.109.887109 [PubMed: 20044514]
17. Popovic ZB, Thomas JD. Assessing observer variability: a user's guide. Cardiovasc Diagn Ther. 2017;7:317–324. doi: 10.21037/cdt.2017.03.12 [PubMed: 28567357]
18. Kim D, Seo JH, Choi KH, Lee SH, Choi JO, Jeon ES, Yang JH. Prognostic Implications of Left Atrial Stiffness Index in Heart Failure Patients With Preserved Ejection Fraction. JACC Cardiovasc Imaging. 2023;16:435–445. doi: 10.1016/j.jcmg.2022.11.002 [PubMed: 36752431]
19. Colazzo F, Castiglioni L, Sironi L, Fontana L, Nobili E, Franzosi M, Guerrini U. Murine left atrium and left atrial appendage structure and function: echocardiographic and morphologic evaluation. PLoS One. 2015;10:e0125541. doi: 10.1371/journal.pone.0125541 [PubMed: 25928887]
20. Medrano G, Hermosillo-Rodriguez J, Pham T, Granillo A, Hartley CJ, Reddy A, Osuna PM, Entman ML, Taffet GE. Left Atrial Volume and Pulmonary Artery Diameter Are Noninvasive Measures of Age-Related Diastolic Dysfunction in Mice. J Gerontol A Biol Sci Med Sci. 2016;71:1141–1150. doi: 10.1093/gerona/glv143 [PubMed: 26511013]
21. Granillo A, Pena CA, Pham T, Pandit LM, Taffet GE. Murine Echocardiography of Left Atrium, Aorta, and Pulmonary Artery. J Vis Exp. 2017. doi: 10.3791/55214
22. Thomas L, Muraru D, Popescu BA, Sitges M, Rosca M, Pedrizzetti G, Henein MY, Donal E, Badano LP. Evaluation of Left Atrial Size and Function: Relevance for Clinical Practice. J Am Soc Echocardiogr. 2020;33:934–952. doi: 10.1016/j.echo.2020.03.021 [PubMed: 32762920]
23. Thomas L, Marwick TH, Popescu BA, Donal E, Badano LP. Left Atrial Structure and Function, and Left Ventricular Diastolic Dysfunction: JACC State-of-the-Art Review. J Am Coll Cardiol. 2019;73:1961–1977. doi: 10.1016/j.jacc.2019.01.059 [PubMed: 31000000]
24. Sirbu C, Herbots L, D'Hooge J, Claus P, Marciniak A, Langeland T, Bijnens B, Rademakers FE, Sutherland GR. Feasibility of strain and strain rate imaging for the assessment of regional left atrial deformation: a study in normal subjects. Eur J Echocardiogr. 2006;7:199–208. doi: 10.1016/j.euje.2005.06.001 [PubMed: 16054869]
25. Cameli M, Caputo M, Mondillo S, Ballo P, Palmerini E, Lisi M, Marino E, Galderisi M. Feasibility and reference values of left atrial longitudinal strain imaging by two-dimensional speckle tracking. Cardiovasc Ultrasound. 2009;7:6. doi: 10.1186/1476-7120-7-6 [PubMed: 19200402]
26. Vianna-Pinton R, Moreno CA, Baxter CM, Lee KS, Tsang TS, Appleton CP. Two-dimensional speckle-tracking echocardiography of the left atrium: feasibility and regional contraction and relaxation differences in normal subjects. J Am Soc Echocardiogr. 2009;22:299–305. doi: 10.1016/j.echo.2008.12.017 [PubMed: 19258177]
27. Patel RB, Lam CSP, Svedlund S, Saraste A, Hage C, Tan RS, Beussink-Nelson L, Tromp J, Sanchez C, Njoroge J, et al. Disproportionate left atrial myopathy in heart failure with preserved ejection fraction among participants of the PROMIS-HFpEF study. Sci Rep. 2021;11:4885. doi: 10.1038/s41598-021-84133-9 [PubMed: 33649383]
28. Donal E, Lip GY, Galderisi M, Goette A, Shah D, Marwan M, Lederlin M, Mondillo S, Edvardsen T, Sitges M, et al. EACVI/EHRA Expert Consensus Document on the role of multi-modality imaging for the evaluation of patients with atrial fibrillation. Eur Heart J Cardiovasc Imaging. 2016;17:355–383. doi: 10.1093/ehjci/jev354 [PubMed: 26864186]

29. Cho DH, Kim YG, Choi J, Kim HD, Kim MN, Shim J, Choi JI, Kim YH, Shim WJ, Park SM. Atrial Cardiomyopathy with Impaired Functional Reserve in Patients with Paroxysmal Atrial Fibrillation. J Am Soc Echocardiogr. 2022. doi: 10.1016/j.echo.2022.09.012
30. Melenovsky V, Hwang SJ, Redfield MM, Zakeri R, Lin G, Borlaug BA. Left atrial remodeling and function in advanced heart failure with preserved or reduced ejection fraction. Circ Heart Fail. 2015;8:295–303. doi: 10.1161/CIRCHEARTFAILURE.114.001667 [PubMed: 25593126]
31. Reddy YNV, Obokata M, Verbrugge FH, Lin G, Borlaug BA. Atrial Dysfunction in Patients With Heart Failure With Preserved Ejection Fraction and Atrial Fibrillation. J Am Coll Cardiol. 2020;76:1051–1064. doi: 10.1016/j.jacc.2020.07.009 [PubMed: 32854840]
32. Ohtani K, Yutani C, Nagata S, Koretsune Y, Hori M, Kamada T. High prevalence of atrial fibrosis in patients with dilated cardiomyopathy. J Am Coll Cardiol. 1995;25:1162–1169. doi: 10.1016/0735-1097(94)00529-y [PubMed: 7897130]
33. Everett THt, Olgin JE. Atrial fibrosis and the mechanisms of atrial fibrillation. Heart Rhythm. 2007;4:S24–27. doi: 10.1016/j.hrthm.2006.12.040 [PubMed: 17336879]
34. Hoit BD. Left Atrial Reservoir Strain: Its Time Has Come. JACC Cardiovasc Imaging. 2022;15:392–394. doi: 10.1016/j.jcmg.2021.10.003 [PubMed: 34801456]
35. Pathan F, D'Elia N, Nolan MT, Marwick TH, Negishi K. Normal Ranges of Left Atrial Strain by Speckle-Tracking Echocardiography: A Systematic Review and Meta-Analysis. J Am Soc Echocardiogr. 2017;30:59–70 e58. doi: 10.1016/j.echo.2016.09.007 [PubMed: 28341032]
36. Singh A, Carvalho Singulane C, Miyoshi T, Prado AD, Addetia K, Bellino M, Daimon M, Gutierrez Fajardo P, Kasliwal RR, Kirkpatrick JN, et al. Normal Values of Left Atrial Size and Function and the Impact of Age: Results of the World Alliance Societies of Echocardiography Study. J Am Soc Echocardiogr. 2022;35:154–164 e153. doi: 10.1016/j.echo.2021.08.008 [PubMed: 34416309]
37. Santos AB, Roca GQ, Claggett B, Sweitzer NK, Shah SJ, Anand IS, Fang JC, Zile MR, Pitt B, Solomon SD, et al. Prognostic Relevance of Left Atrial Dysfunction in Heart Failure With Preserved Ejection Fraction. Circ Heart Fail. 2016;9:e002763. doi: 10.1161/CIRCHEARTFAILURE.115.002763 [PubMed: 27056882]
38. Kusunose K, Penn MS, Zhang Y, Cheng Y, Thomas JD, Marwick TH, Popovic ZB. How similar are the mice to men? Between-species comparison of left ventricular mechanics using strain imaging. PLoS One. 2012;7:e40061. doi: 10.1371/journal.pone.0040061 [PubMed: 22768220]
39. Matsiukevich D, Kovacs A, Li T, Kokkonen-Simon K, Matkovich SJ, Oladipupo S, Ornitz Dm Md P. Characterization of a robust mouse model of heart failure with preserved ejection fraction. Am J Physiol Heart Circ Physiol. 2023. doi: 10.1152/ajpheart.00038.2023
40. Yoshida Y, Nakanishi K, Daimon M, Ishiwata J, Sawada N, Hirokawa M, Kaneko H, Nakao T, Mizuno Y, Morita H, et al. Association of arterial stiffness with left atrial structure and phasic function: a community-based cohort study. J Hypertens. 2020;38:1140–1148. doi: 10.1097/HJH.0000000000002367 [PubMed: 32371804]
41. Kurt M, Wang J, Torre-Amione G, Nagueh SF. Left atrial function in diastolic heart failure. Circ Cardiovasc Imaging. 2009;2:10–15. doi: 10.1161/CIRCIMAGING.108.813071 [PubMed: 19808559]
42. Forrester SJ, Booz GW, Sigmund CD, Coffman TM, Kawai T, Rizzo V, Scalia R, Eguchi S. Angiotensin II Signal Transduction: An Update on Mechanisms of Physiology and Pathophysiology. Physiol Rev. 2018;98:1627–1738. doi: 10.1152/physrev.00038.2017 [PubMed: 29873596]
43. Bapat A, Schloss MJ, Yamazoe M, Grune J, Hulsmans M, Milan DJ, Nahrendorf M, Ellinor PT. A Mouse Model of Atrial Fibrillation in Sepsis. Circulation. 2023;147:1047–1049. doi: 10.1161/CIRCULATIONAHA.122.060317 [PubMed: 36972346]
44. Aschar-Sobbi R, Izaddoustdar F, Korogyi AS, Wang Q, Farman GP, Yang F, Yang W, Dorian D, Simpson JA, Tuomi JM, et al. Increased atrial arrhythmia susceptibility induced by intense endurance exercise in mice requires TNFalpha. Nat Commun. 2015;6:6018. doi: 10.1038/ncomms7018 [PubMed: 25598495]
45. Hao Y, Tsuruda T, Sekita-Hatakeyama Y, Kurogi S, Kubo K, Sakamoto S, Nakamura M, Udagawa N, Sekimoto T, Hatakeyama K, et al. Cardiac hypertrophy is exacerbated in aged mice lacking

the osteoprotegerin gene. Cardiovasc Res. 2016;110:62–72. doi: 10.1093/cvr/cvw025 [PubMed: 26825553]

46. Toth P, Tarantini S, Springo Z, Tucsek Z, Gautam T, Giles CB, Wren JD, Koller A, Sonntag WE, Csiszar A, et al. Aging exacerbates hypertension-induced cerebral microhemorrhages in mice: role of resveratrol treatment in vasoprotection. Aging Cell. 2015;14:400–408. doi: 10.1111/acel.12315 [PubMed: 25677910]
47. Gevaert AB, Shakeri H, Leloup AJ, Van Hove CE, De Meyer GRY, Vrints CJ, Lemmens K, Van Craenenbroeck EM. Endothelial Senescence Contributes to Heart Failure With Preserved Ejection Fraction in an Aging Mouse Model. Circ Heart Fail. 2017;10. doi: 10.1161/CIRCHEARTFAILURE.116.003806
48. Jansen HJ, Moghtadaei M, Rafferty SA, Rose RA. Atrial Fibrillation in Aging and Frail Mice: Modulation by Natriuretic Peptide Receptor C. Circ Arrhythm Electrophysiol. 2021;14:e010077. doi: 10.1161/CIRCEP.121.010077 [PubMed: 34490788]
49. Verheule S, Sato T, Everett Tt, Engle SK, Otten D, Rubart-von der Lohe M, Nakajima HO, Nakajima H, Field LJ, Olgin JE. Increased vulnerability to atrial fibrillation in transgenic mice with selective atrial fibrosis caused by overexpression of TGF-beta1. Circ Res. 2004;94:1458–1465. doi: 10.1161/01.RES.0000129579.59664.9d [PubMed: 15117823]
50. Fu F, Pietropaolo M, Cui L, Pandit S, Li W, Tarnavski O, Shetty SS, Liu J, Lussier JM, Murakami Y, et al. Lack of authentic atrial fibrillation in commonly used murine atrial fibrillation models. PLoS One. 2022;17:e0256512. doi: 10.1371/journal.pone.0256512 [PubMed: 34995278]
51. Negishi K. Incremental Diagnostic Value of Left Atrial Strain Over Left Atrial Volume: An Analogy of Glucose Level and Glycosylated Hemoglobin? JACC Cardiovasc Imaging. 2018;11:1416–1418. doi: 10.1016/j.jcmg.2017.10.011 [PubMed: 29153566]
52. Hanley MJ, Abernethy DR, Greenblatt DJ. Effect of obesity on the pharmacokinetics of drugs in humans. Clin Pharmacokinet. 2010;49:71–87. doi: 10.2165/11318100-000000000-00000 [PubMed: 20067334]

Clinical Perspective

Accumulating clinical evidence suggests that atrial myopathy may be the underlying pathophysiology that explains the adverse cardiovascular outcomes in heart failure and atrial fibrillation. Impaired left atrial function identified by echocardiographic based strain imaging has emerged as a key measure of atrial myopathy. Here, we address an important knowledge gap by describing the quantification of left atrial function in preclinical mouse models of atrial myopathy by speckle-tracking echocardiography. Establishment of left atrial strain imaging in mice provides the field with a timely platform to examine underlying pathophysiologic mechanisms and to develop novel therapies for atrial myopathy.

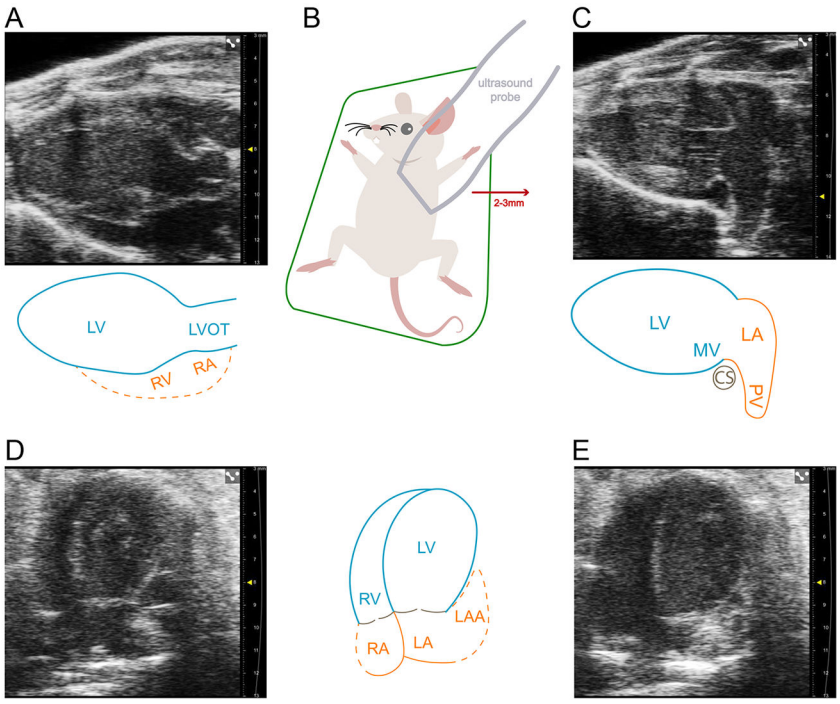

Figure 1. Current methods of examining the murine left atrium are inadequate

(A) Parasternal long axis view of the left ventricle (LV), LV outflow tract, and with partial view of the right ventricle (RV) and right atrium (RA). This is where left atrial (LA) size is commonly measured. **(B)** The modified parasternal long axis view, revealing the LA proper, can be achieved by moving the ultrasound probe laterally to the left by 2-3 mm. **(C)** Modified parasternal long axis view that displays the LA proper and one of three pulmonary veins. **(D)** Apical four chamber view during atrial diastole displaying the LA and partially obscured left atrial appendage (LAA). Optimization of the probe angle is difficult in this probe position due to the size of the ultrasound probe compared to the mouse thorax. **(E)** Apical four chamber view during atrial systole displaying a further obscured view of the LA and LAA. The obscured view of the LA and LAA limits the ability to track speckles in this echocardiographic window. Dotted lines in the figure indicate indeterminate anatomical borders. Scale marks indicate 1 millimeter.

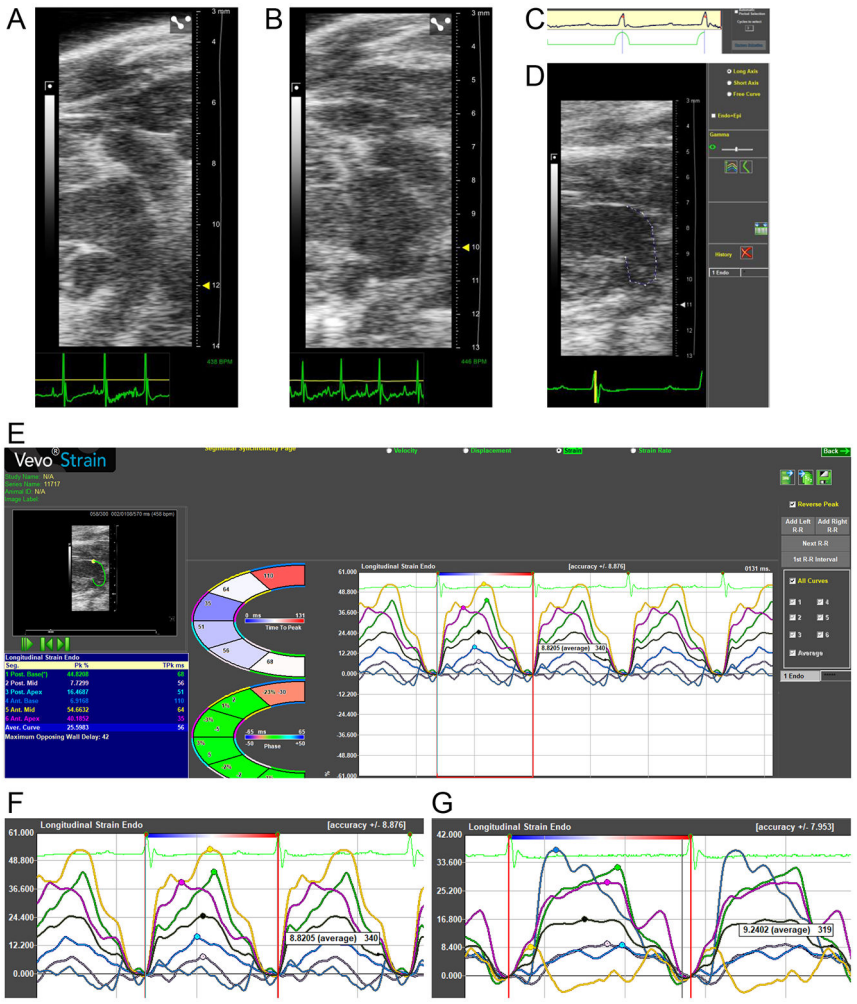

Figure 2. Measurement of LA function in mice by speckle-tracking echocardiography

(A) Representative image and Video 1 of a left atrium (LA) from a young mouse. **(B)** Representative image and Video 2 of an LA from an AngII mouse. **(C)** In the software package to measure strain the period selection is kept at the default R-R interval so that LA reservoir strain is entirely positive through one cardiac cycle. **(D)** The long axis curve tool is utilized to draw a line between the anterior and posterior mitral valve annulus. This adapts the software, originally designed to measure LV strain, to calculate LA strain instead. **(E)** The Time-to-Peak software package is selected, with the “Reverse Peak” box checked, to calculate LA strain. The LA is divided automatically into six strain segments, but only the black-colored average curve values are utilized. LA contractile strain can be identified by the second peak following the P wave on ECG. LA conduit strain is calculated as the difference between LA reservoir and contractile strain. **(F)** Representative LA strain curves from a young mouse. **(G)** Representative LA strain curves from a HFpEF mouse.

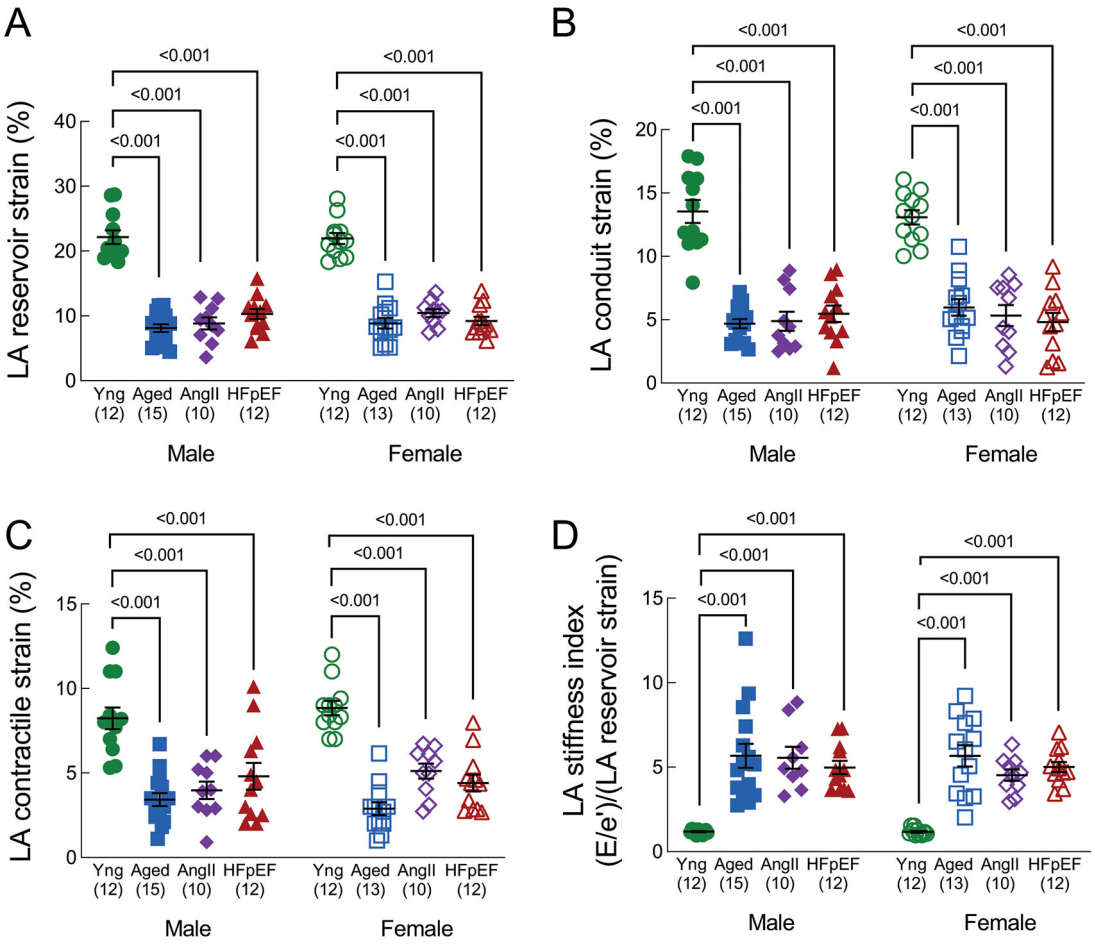

Figure 3. Left atrial function

(A) LA reservoir strain, **(B)** LA conduit strain, **(C)** LA contractile strain, and **(D)** LA stiffness index, defined as E/e' divided by LA reservoir strain %. A lower strain % represents worse mechanical function. LA conduit and contractile strain are presented as absolute values. Data in are mean±SEM and outcomes for each sex were analyzed by one-way ANOVA with Tukey's multiple comparisons test. A primary interaction *P* value < 0.05 was considered significant, and significant differences identified by the post-test are indicated.

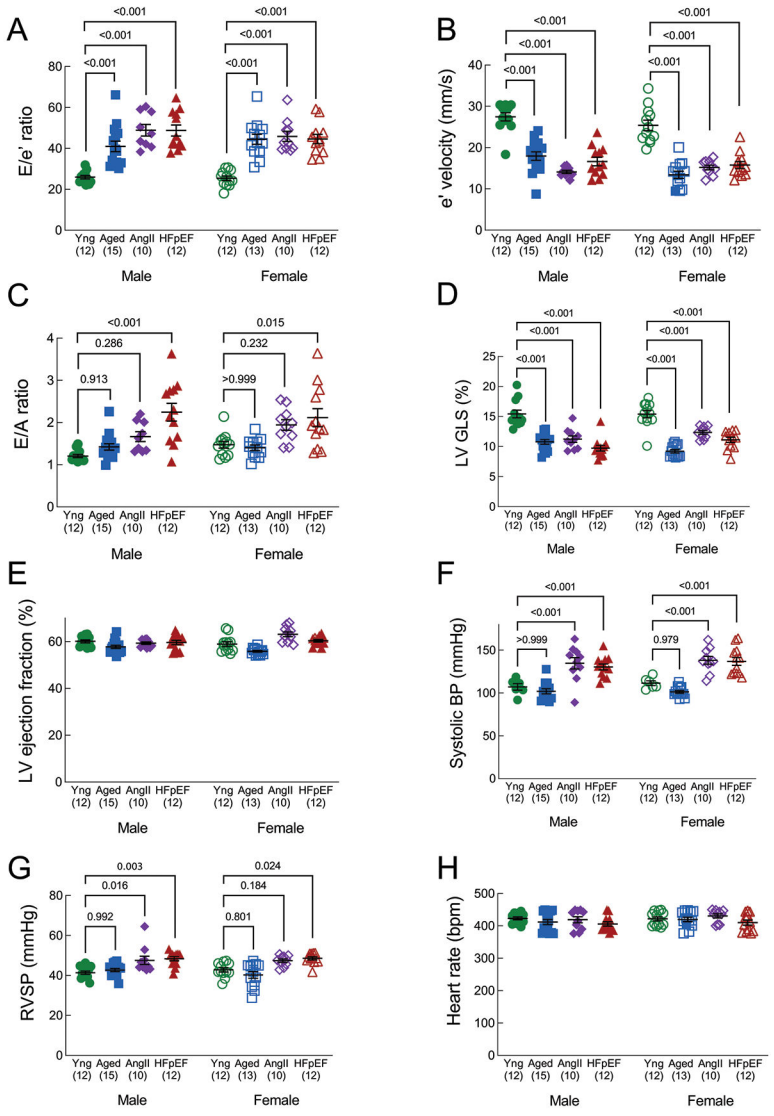

Figure 4. Left ventricular function

(A) E/e' ratio (septal); higher E/e' indicates worse diastolic function. **(B)** e' velocity (mm/s); lower e' is associated with worse diastolic function. **(C)** E/A ratio; higher E/A ratio indicates worse diastolic function. **(D)** LV global longitudinal strain, presented as an absolute value. Higher strain indicates higher function. **(E)** LV ejection fraction (systolic function). **(F)** Right ventricular systolic pressure, calculated from pulmonary artery acceleration and ejection times. **(G)** Systolic blood pressure, collected by tail cuff. **(H)** Heart rate, measured by ECG during echocardiography (parasternal long axis view). Data are mean±SEM and outcomes for each sex were analyzed by one-way ANOVA with Tukey's multiple comparisons test. A primary interaction P value < 0.05 was considered significant, and significant differences identified by the post-test are indicated.

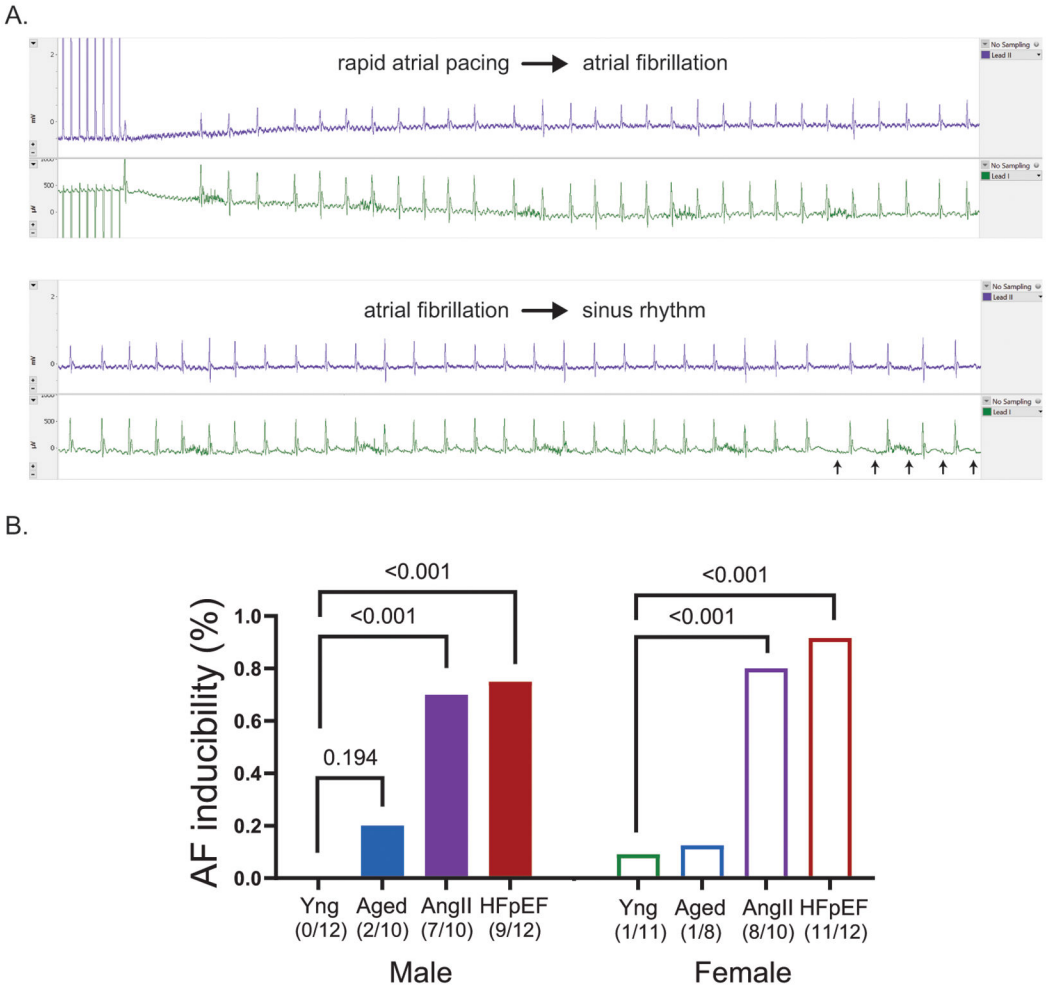

Figure 5. Rapid transesophageal atrial pacing to induce atrial fibrillation

(A) Example surface ECG tracing of a mouse that underwent transesophageal rapid atrial pacing to induce AF, followed by subsequent reversion to sinus rhythm (P wave denoted by red arrows). **(B)** Percentage and number of mice with inducible AF by transesophageal rapid atrial pacing among the mouse groups. *P* values were calculated by Fisher's exact test.